Original Article

SORPTIVE REMOVAL OF CHLORIDE AND SULPHATE IONS IN WASTEWATER FROM AN ADVANCED CHEMISTRY LABORATORY

Utange[1], P.I. [*], Wuana[2], R.A., and Eneji[3], I.S.

[1]Centre for Food Research and Technology, Rev Fr Moses Orshio Adasu University (Formerly Benue State University), Makurdi – Nigeria

[2]Department of Chemistry, Joseph Sarwuan Tarka University, Makurdi – Nigeria

[3]Department of Chemistry, Joseph Sarwuan Tarka University, Makurdi – Nigeria

*Corresponding Author: putange@bsum.edu.ng

ABSTRACT

The removal of chloride and sulphate ions in wastewater from an advanced chemistry multipurpose laboratory was conducted using activated carbon adsorbents from seed shells of Irvingia gabonensis (CIG150 = 150 µm and CIG300 = 300 µm particle size) and a commercial activated carbon (CAC). Chloride and sulphate ions were quantified using turbidimetric method. Adsorption experiments were conducted in batch mode considering the effect of pH, adsorbent dosage, contact time and isotherms. The optimum adsorption capacity for the adsorption of chloride ions onto CIG150 and CIG300 were 4.973 and 5.392 mg/g at pH 6.8 respectively while CAC recorded 3.147 mg/g at pH 7.6; CIG300 and CAC recorded 2.892 and 3.145 mg/g for the adsorption of sulphate at pH 7.7 while the sulphate-CIG150 adsorption system recorded optimum adsorption capacity of 2.526 mg/g at pH 8.1. Langmuir isotherm fitted the equilibrium data for the adsorption studies. Chloride ions recorded Langmuir maximum adsorption capacity, (mg/g) for CIG150, CIG300 and CAC as 2.6998, 2.8637, 2.8794 at 298 K; 2.7824, 2.9718, 2.9745 at 303 K and 2.8802, 3.0572, 3.1133 at 308 K respectively. Similarly, sulphate ions recorded (mg/g) as 1.3738, 1.3144, 1.4835 at 298 K; 1.4223, 1.4118, 1.5456 at 303 K; 1.4923, 1.5158, 1.6345 at 308 K. The calculated thermodynamic quantities indicate that, the adsorption process for the uptake of chloride and sulphate ions were spontaneous, exothermic and characteristic of physical adsorption. The Weber-Morris intra-particle kinetic model explained the adsorption process. Activated carbon from Irvingia gabonensis seed shells was thus recommended for real wastewater treatment.

KEYWORDS: Sorptive Removal, Chloride, Sulphate, Wastewater, Irvingia Gabonensis, Adsorption Isotherms, Kinetic Models, Thermodynamics

Open Access
Correspondence;

Citation: *P.I. Utange, R.A. Wuana, and I.S. Eneji (2026) Sorptive Removal of Chloride and Sulphate Ions in Wastewater from an Advanced Chemistry Laboratory*

Date of Publication:
Vol. 9 (1), 2026

pp 210-229

INTRODUCTION

Laboratory waste management is essential for protecting human health, laboratory personnel, and the environment. Chemistry laboratory wastes can be classified into hazardous and non-hazardous wastes and may occur as liquids, sludge, solids, and gaseous emissions. Proper management and disposal are necessary to minimize environmental pollution, protect human health, and promote sustainable laboratory operations (Sahar, 2019). Laboratory wastewater may contain suspended, colloidal, and dissolved organic and inorganic substances, with its composition depending largely on the activities and materials involved in the laboratory processes (Berehanu *et al*., 2015; Phifer, 2024). Its characteristics may include variations in solids, colour, odour, turbidity, temperature, acidity/alkalinity, nutrients, salts, organic compounds, and potentially toxic substances (Spellman, 2020).

In developing countries such as Nigeria, laboratory wastewater is frequently discharged through sinks into septic tanks or soak-away systems without adequate pre-treatment. This practice may result in the migration of contaminants into soil and groundwater and consequently pose risks to human health and the environment (Ehalt-Macedo *et al*., 2022). Of particular concern are inorganic ions such as chloride, sulphate, phosphate and nitrate, which commonly occur in groundwater but may indicate anthropogenic influence when present at elevated concentrations (Utange *et al*., 2021). Chloride can also serve as an indicator of contamination associated with septic systems (Omowumi, 2018).

Sulphate occurs naturally in minerals but may also enter water through industrial discharges and atmospheric deposition. Elevated concentrations are particularly associated with groundwater. Although current evidence does not establish a specific sulphate concentration in drinking water that is likely to cause adverse health effects, concentrations around 1,000 – 1,200 mg/L have been associated with laxative effects, particularly in the presence of calcium and magnesium. Sulphate may also impart taste to drinking water and contribute to corrosion of water-distribution systems (WHO, 2026).

Both chloride and sulphate ions can influence the corrosion behaviour of metals and cementitious materials. Chloride is particularly important because it can disrupt protective passive films on metals and promote localized forms of corrosion such as pitting and crevice corrosion (Cui *et al*., 2019; Song *et al*., 2017; Zhou *et al*., 2018). Sulphate can also promote corrosion under certain conditions, although its effect depends on concentration and the surrounding chemical environment. Studies have shown that sulphate may accelerate general corrosion of reinforcing steel at sufficiently high concentrations, while under some conditions it may reduce corrosion through the formation of protective deposits (Dong *et al*., 2017; Bernardi *et al*., 2020). The relative effects of chloride and sulphate ions are therefore influenced by factors such as pH, concentration, and the chloride-to-sulphate ratio (Cao *et al*., 2013; Ismail, 2014).

Several technologies are available for removing contaminants from wastewater, including chemical precipitation, ion exchange, adsorption, membrane filtration, coagulation – flocculation, flotation, and electrochemical treatment (Zhang *et al*., 2014; Al-Qahtani, 2016). Among these techniques, adsorption is considered an attractive wastewater-treatment method because of its relatively low initial cost, low energy requirement, operational simplicity, potential for adsorbent regeneration, and availability of suitable precursor materials (Somashekara & Mulky, 2023).

Against this background, the present study explores the use of carbon prepared from *Irvingia gabonensis* seed shells for the removal of chloride and sulphate ions from wastewater. The precursor material had previously been prepared and characterized and was reported to possess properties favourable for use as an adsorbent (Utange *et al*., 2021). The study therefore investigates the potential of this locally available agricultural biomass – derived carbon as a sustainable adsorbent for wastewater treatment.

MATERIALS AND METHODS

Adsorption Experiments

Mixed methodology was adopted in the study using the approach described by Utange *et al.* (2021) where CIG150 and CIG300 were carbon from *Irvingia gabonensis* seed shell of pore size150 and 300 µm respectively while CAC was a commercial activated carbon). Batch adsorption experiments were then conducted to investigate the effect of initial solution pH at 298 K, adsorbent dosage and contact time at different temperatures (K): 298, 303 and 308. Turbidimetric method was employed for the determination of chloride and sulphate ions. Chloride was determined by a modified turbidimetric method based on the precipitation of chloride as silver chloride (AgCl) in an acidic medium containing silver nitrate and polyvinyl alcohol as a stabilizing agent, following the method of Mesquita et al. (2002). The turbidimetric determination of sulphate was adapted from IS 3025 (Part 24), with modifications to the stock and calibration concentrations and sample volume to accommodate the concentration range of the samples (BIS, 2022). The amount of the ions adsorbed was calculated using the mass balance equation (Equation 1). The adsorption experimental data were modelled according to the linear forms of Langmuir (Equation 2), Freundlich (Equation 3), Temkin (Equation 4) and Dubnin-Radushkevich (Equation 5) isotherms. A dimensionless equilibrium parameter called separation factor *[R_L]* (Equation 6) was used to study the applicability of Langmuir isotherm. Modelling of sorption kinetics was also carried out according to the linear forms of Lagergren pseudo-first order (Equation 7), Blanchard pseudo-second order (Equation 8) and Weber-Morris intra-particle diffusion (Equation 9) models.

$$q_e = \frac{(C_o - C_e)V}{m} \tag{1}$$

$$\frac{C_e}{q_e} = \frac{1}{q_m K_L} + \frac{C_e}{q_m} \tag{2}$$

$$\log q_e = \log K_f + \frac{1}{n}\log C_e \tag{3}$$

$$q_e = B\ln A_T + B\ln C_e \tag{4}$$

$$\ln q_e = \ln q_s - K_{DR}\varepsilon^2 \tag{5}$$

$$R_L = \frac{1}{1+(1+K_L C_o)} \tag{6}$$

$$\ln(q_e - q_t) = \ln q_e - k_1 t \quad (7)$$

$$\frac{t}{q_t} = \frac{1}{k_2 q_e^2} + \frac{1}{q_e} t \quad (8)$$

$$q_t = k_{id}\sqrt{t} + C \quad (9)$$

where C_o and C_e are the initial and residual chloride ions concentrations (mg L^{-1}), respectively; V is the aliquot of wastewater used in L; and m is the mass (g) of adsorbent used for a particular batch treatment (Utange *et al.*, 2021).

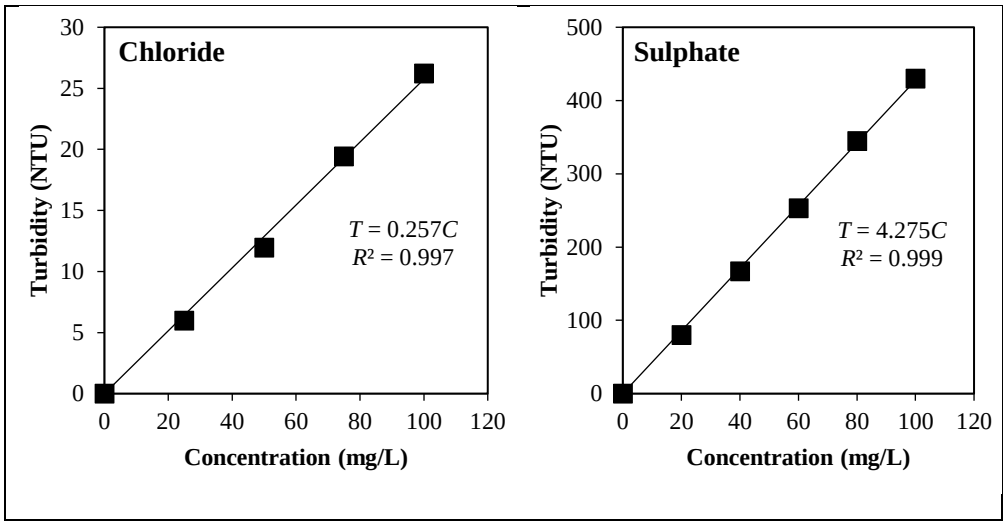


Figure 1: Calibration Curves for Determination of Chloride and Sulphate Ions in Wastewater

RESULTS

Effect of Initial Solution pH on Adsorption of Chloride Ions from Wastewater

The effect of initial solution pH (illustrated in Figure 2), on the sorptive removal of chloride and sulphate ions in wastewater generated from an advanced multipurpose chemistry laboratory using activated carbon derived from seed shells of *Irvingia gabonensis* and a commercial activated carbon (CIG150, CIG300 and CAC) were demonstrated.

At pH value of 3, chloride adsorption was 1.671, 1.869 and 1.204 mg/g for CIG150, CIG300 and CAC respectively. As pH was increased, the maximum adsorption capacity of 4.973, 5.392 and 3.147 was achieved for CIG150, CIG300 and CAC at pH 7. Further increase in the solution pH led to a decrease in the adsorption capacity. The efficiency of these adsorbents for the removal of chloride ions was in the order of CIG300>CIG150>CAC with optimum pH of 7.6 for CAC and 6.8 for both CIG150 and CIG 300.

However, at pH of 3, sulphate uptake was 0.889, 0.974 and 1.227 mg/g for CIG150, CIG300 and CAC respectively. As pH was increased, CIG150 recorded maximum adsorption of sulphate at pH 9 (2.526 mg/g), further increase led to a decrease in the adsorption capacity, while CIG300 and CAC recorded increased adsorption capacity to a maximum of 2.892 and 3.145 at pH 7, further increase in pH recorded decreased adsorption capacity. The efficiency of the adsorbents for the removal of sulphate ions was in the order of CAC >CIG300>CIG150 with optimum pH of 8.1 for CIG150 and 7.7 for both CIG300 and CAC.

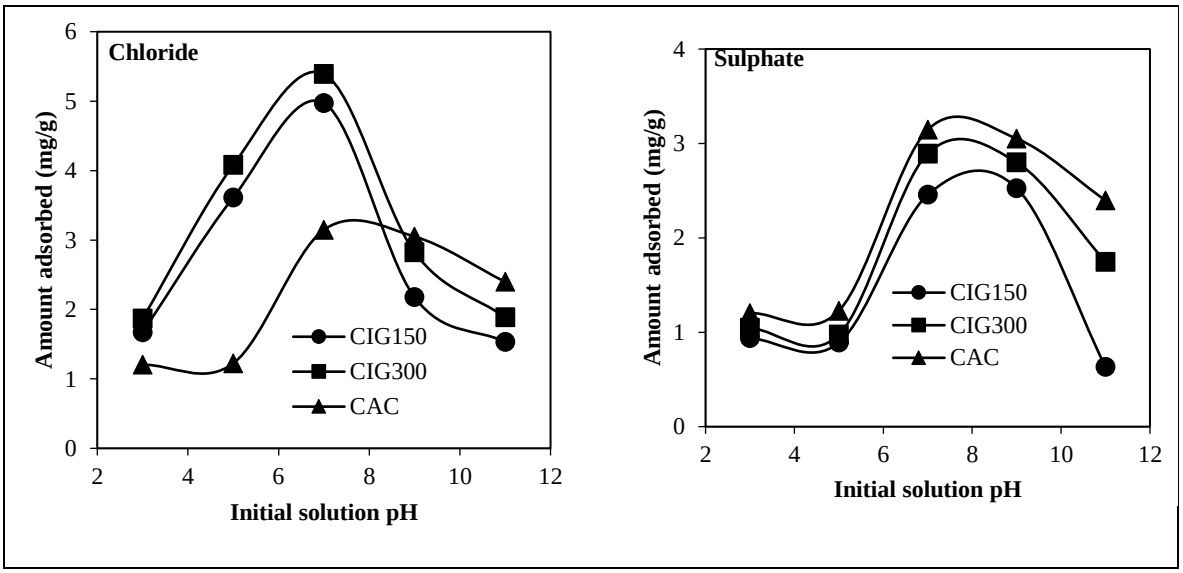


Figure 2: Effect of Initial Solution pH on Removal of Chloride and Sulphate Ions from Wastewater by I. gabonensis Seed Shells Carbon (CIG150 = 150 µm; CIG300 = 300 µm Particle Size) and Commercial Activated Carbon (CAC)

Effect of Adsorbent Dosage on Adsorption of Chloride and Sulphate Ions in Wastewater

The effect of adsorbent dosage on the sorptive removal of chloride and sulphate ions in wastewater from a multipurpose chemistry laboratory using activated carbon derived from seed shells of *Irvingia gabonensis* and a commercial activated carbon at different temperatures are presented in Figures 3 – 4.

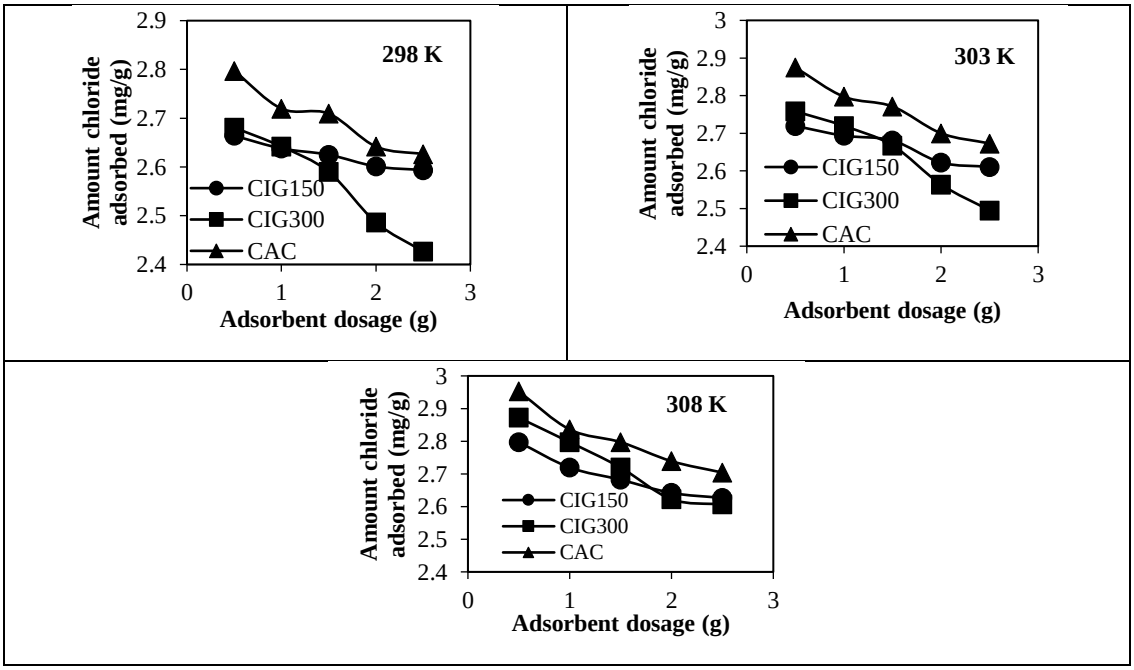


Figure 3: Effect of Adsorbent Dosage on Chloride Ions Removal from Wastewater by I. gabonensis Seed Shells Carbon (CIG150 = 150 µm; CIG300 = 300 µm Particle Size) and Commercial Activated Carbon (CAC) at different Temperatures

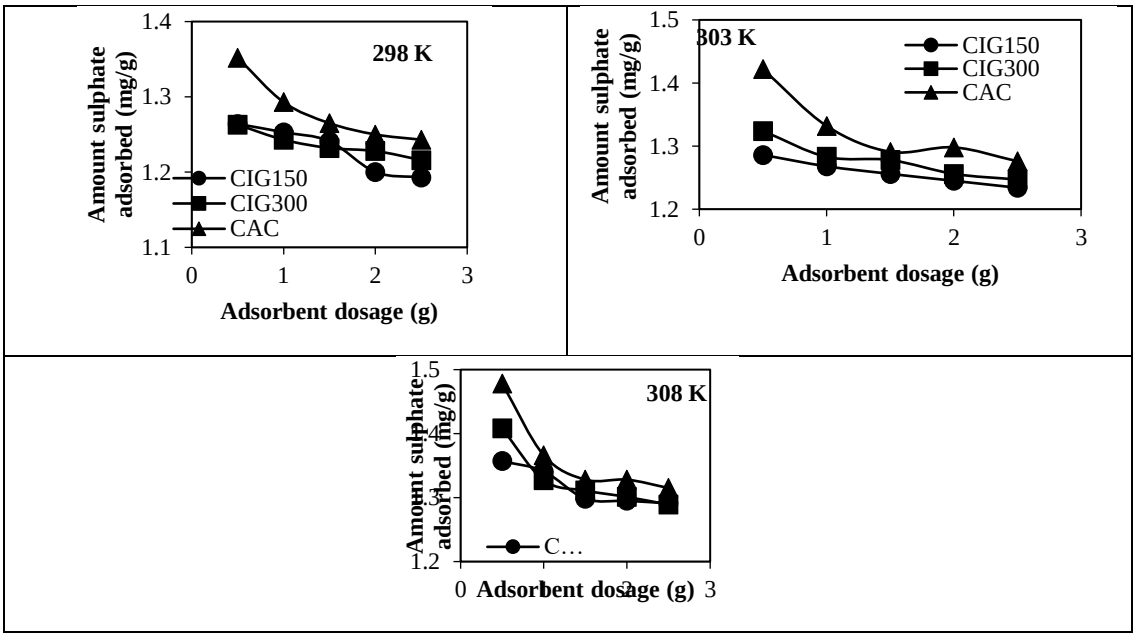


Figure 4: Effect of Adsorbent Dosage on Sulphate Removal from Wastewater by I. gabonensis Seed Shells Carbon (CIG150 = 150 µm; CIG300 = 300 µm Particle Size) and Commercial Activated Carbon (CAC) at different Temperatures

Langmuir Isotherm Models for Adsorption of Chloride and Sulphate Ions

The equilibrium data for the adsorption of chloride and sulphate ions in wastewater from a multipurpose chemistry laboratory using activated carbon derived from seed shells of *Irvingia gabonensis* and a commercial activated carbon (CIG150, CIG300 and CAC) at different temperatures were fitted into the linearized forms of the Langmuir, Freundlich, Temkin and Dubinin-Radushkevich models. Out of these, only the Langmuir Isotherm fitted well the data obtained and the isotherm parameters in Table 1.

Table 1: Langmuir Isotherm Parameters for Adsorption of Chloride and Sulphate Ions on Carbonized Irvingia gabonensis Seed Shells (CIG150 and CIG300) and Commercial Adsorbent (CAC) at Different Temperatures

Anion	Adsorbent	Model	298K	303K	308K
Cl^-	CIG150	Q_m (mg.g^{-1})	2.6998	2.7824	2.8802
		K_L (L.mg^{-1})	0.7702	0.5133	0.3355
		K_L ($\times 10^4$ L.mol^{-1})	2.7307	1.8197	1.1893
		R^2	0.9999	0.9998	0.9988
		R_L	0.0247	0.0361	0.0533
	CIG300	Q_m (mg.g^{-1})	2.8637	2.9718	3.0572
		K_L (L.mg^{-1})	0.1838	0.1716	0.1512
		K_L ($\times 10^3$ L.mol^{-1})	6.5155	6.0824	5.3608
		R^2	0.9994	0.9991	0.9985
		R_L	0.0894	0.0945	0.1046
	CAC	Q_m (mg.g^{-1})	2.8794	2.9718	3.1133
		K_L (L.mg^{-1})	0.3365	0.3064	0.2604
		K_L ($\times 10^4$ L.mol^{-1})	1.1931	1.0862	0.9231
		R^2	0.9990	0.9991	0.9979

		R_L	0.0531	0.0577	0.0666
SO_4^{2-}	CIG150	Q_m (mg.g^{-1})	1.3738	1.4223	1.4923
		K_L (L.mg^{-1})	0.2213	0.2102	0.2028
		K_L ($\times 10^4$ L.mol^{-1})	2.1259	2.0190	1.9477
		R^2	0.9991	0.9979	0.9996
		R_L	0.0765	0.0618	0.0483
	CIG300	Q_m (mg.g^{-1})	1.3144	1.4118	1.5158
		K_L (L.mg^{-1})	0.4126	0.2471	0.1897
		K_L ($\times 10^5$ L.mol^{-1})	3.9636	2.3735	1.8224
		R^2	0.9993	0.9976	0.9897
		R_L	0.0442	0.0697	0.0871
	CAC	Q_m (mg.g^{-1})	1.4835	1.5456	1.6345
		K_L (L.mg^{-1})	0.1661	0.1536	0.1391
		K_L ($\times 10^5$ L.mol^{-1})	1.5951	1.4752	1.3361
		R^2	0.9929	0.9823	0.9815
		R_L	0.0971	0.1033	0.1117

Thermodynamics of Adsorption of Chloride and Sulphate

Gibbs free energy change (ΔG^o), enthalpy change (ΔH^o), entropy (ΔS^o) for the adsorption of chloride and sulphate ions in wastewater from a multipurpose chemistry laboratory using activated carbon produced from seed shells of *Irvingia gabonensis* and a commercial activated carbon (CIG150, CIG300 and CAC) were determined by evaluation of K_L at different temperatures. The Gibbs free energy change was calculated using:

$$\Delta G^o = -RT \ln K_L \quad (10)$$

where R is the universal gas constant (8.314 J/mol.K), T is the temperature (K), K_L (L/mol) is the Langmuir affinity constant. Since the values of K_L were obtained L/mg, they were converted to L/mol with the aid of Eq. 11:

$$K_L\,(\text{L/mol}) = K_L\,(\text{L/mg}) \times 10^3\,(\text{mg/g}) \times f_w\,(\text{g/mol}) \quad (11)$$

where f_w is the formula weight of chloride and sulphate (35.453 and 96.0576 g/mol, respectively).

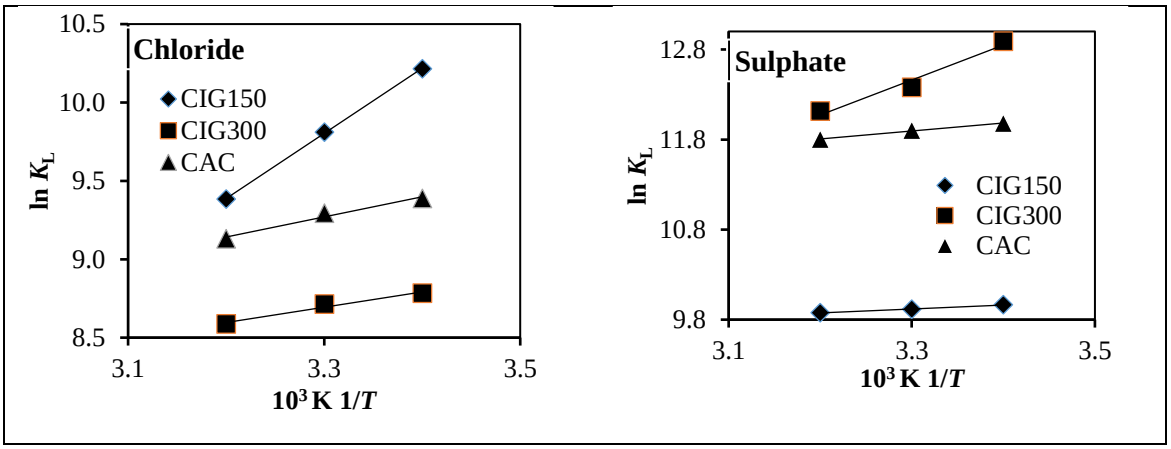


Figure 5: Van't Hoff Plots for Aqueous Phase Removal of Chloride and Sulphate Ions

Enthalpy (ΔH^o) and entropy (ΔS^o) evaluated from the slope and intercept of the $\ln K_L$ (L/mol) versus (10^3 K)/T plots as presented in Figure6 from the Van't Hoff equation:

$$\ln K_L = \frac{\Delta S^o}{R} - \frac{\Delta H^o}{RT} \quad (12)$$

where R and T keep their definitions in Eq. 10 (Utange *et al.*, 2021). The thermodynamic parameters evaluated for the aqueous phase removal of the chloride and sulphate ions by CIG150, CIG300 and CAC are summarized in Table 2.

Table 2: Evaluated Thermodynamic Parameters for Adsorption of Chloride and Sulphate Ions by I. gabonensis Seed Shells Carbon (CIG150 = 150 µm; CIG300 = 300 µm Particle Size) and Commercial Activated Carbon (CAC) at Different Temperatures

Adsorbent	***T* (*K*)**	**ΔG^o (kJ mol^{-1})**	**ΔH^o (kJ mol^{-1})**	**ΔS^o(JK^{-1}mol^{-1})**
Chloride – CIG150			-34.5530	-32.5252
	298	-25.308		
	303	-24.710		
	308	-24.029		
Chloride – CIG300			-8.1094	45.5216
	298	-21.758		
	303	-21.950		
	308	-21.988		
Chloride – CAC			-10.6660	41.8742
	298	-23.257		
	303	-23.380		
	308	-23.410		
Sulphate – CIG150			-3.6390	70.4495
	298	-24.688		
	303	-24.972		
	308	-25.292		
Sulphate – CIG300			-32.2999	-2.9955
	298	-31.018		
	303	-31.180		
	308	-31.936		
Sulphate – CAC			-7.365372	74.5873
	298	-29.681		
	303	-29.982		
	308	-30.223		

Adsorption rate curves and kinetic models

The plots in Figures 6 – 7 illustrate rate curves for the removal of chloride and sulphate ions in wastewater from a multipurpose chemistry laboratory using activated carbon derived from seed shells of *Irvingia gabonensis* and a commercial activated carbon at different temperatures.

From the rate curves for the adsorption of chloride and sulphate ions onto CIG150, CIG300 and CAC, the adsorption capacity increased as time was increased from 10 minutes to 240 minutes. But for all chloride-adsorbent systems at 308 K, Chloride-CIG300, Chloride-CAC at 303 K and all sulphate-adsorbent sorption systems, the uptake of these anions increased very rapidly in the first 10 minutes and then slowed down thereby increasing marginally in its uptake. The scenario however changed with chloride-adsorbent systems at 298k and chloride-CIG150 at 303 K where there was rapid uptake of chloride up to 30 minutes

before slowing down and the marginal increase in the uptake chloride ions set in. Generalising, the adsorption efficiency/potency of the adsorbents was in the order of CAC>CIG300>CIG150 at all the temperatures studied.

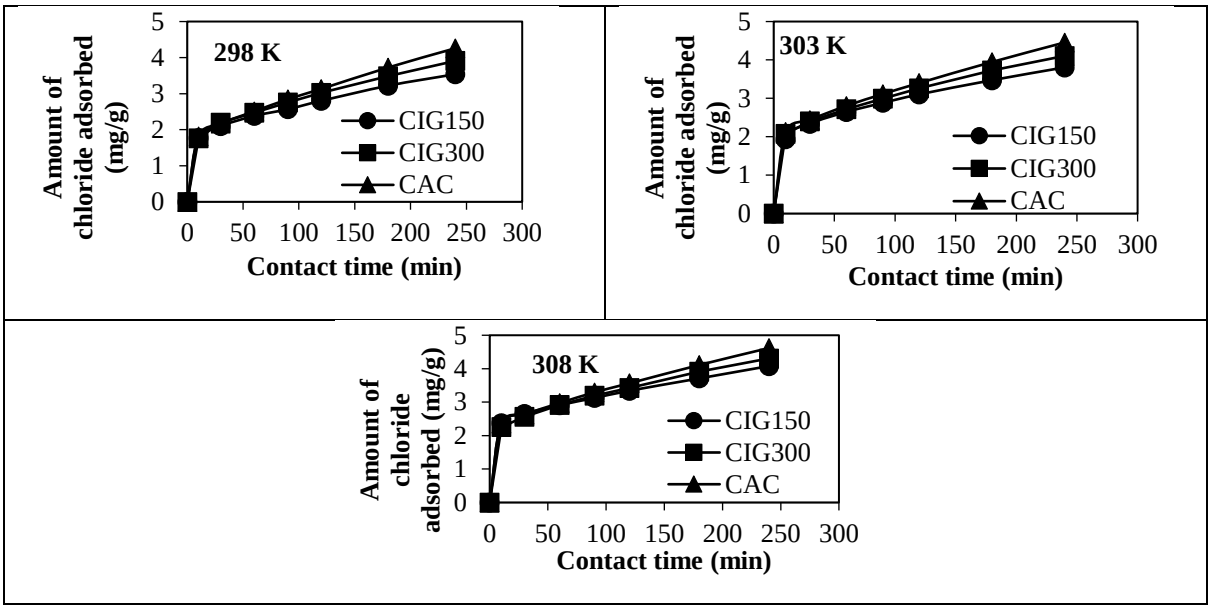


Figure 6: Rate Curves for Removal of Chloride Ions from Wastewater by I. gabonensis Seed Shells Carbon (CIG150 = 150 µm; CIG300 = 300 µm Particle Size) and Commercial Activated Carbon (CAC)

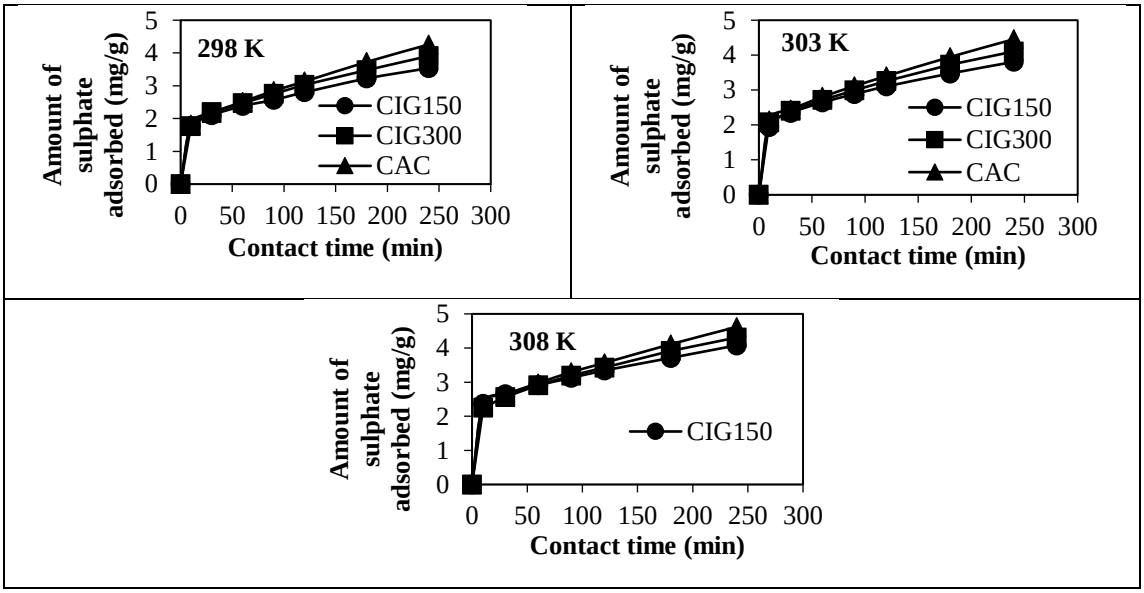


Figure 7: Rate Curves for Removal of Sulphate Ions from Wastewater by I. gabonensis Seed Shells Carbon (CIG150 = 150 µm; CIG300 = 300 µm Particle Size) and Commercial Activated Carbon (CAC)

The experimental data for the adsorption of chloride and sulphate ions in wastewater from a multipurpose chemistry laboratory using activated carbon derived from seed shells of *Irvingia gabonensis* and a commercial activated carbon at different

temperatures were fitted into the linear forms of Lagergren pseudo-first order, Blanchard pseudo-second order and the Weber-Morris intra-particle diffusion kinetic models. The kinetic plots for the removal of these anions are shown in Figures 8 – 9 and the kinetic parameters summarized in Table 3.

The range of kinetic parameters for chloride-CIG150 sorption system were recorded thus: $0.91 \leq k_1(\times 10^{-2}) \leq 0.99$, $0.943 \leq k_2(\times 10^{-2}) \leq 1.078$, $13.68 \leq k_{id}(\times 10^{-2}) \leq 14.90$across the temperatures. In the same fashion, the chloride-CIG300 sorption system recorded the kinetic parameters in the order of $0.88 \leq k_1(\times 10^{-2}) \leq 0.92$, $0.728 \leq k_2(\times 10^{-2}) \leq 0.813$, $16.56 \leq k_{id}(\times 10^{-2}) \leq 17.05$ while the chloride-CAC sorption system recorded $0.65 \leq k_1(\times 10^{-2}) \leq 0.67$, $0.544 \leq k_2(\times 10^{-2}) \leq 0.671$, $18.38 \leq k_{id}(\times 10^{-2}) \leq 19.72$.

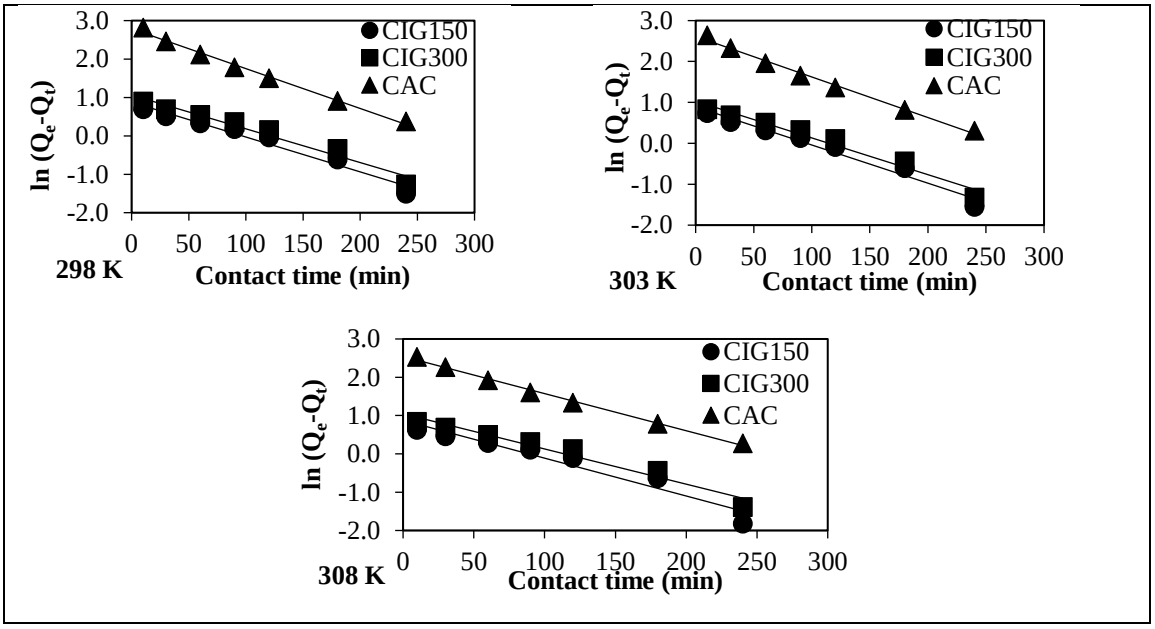
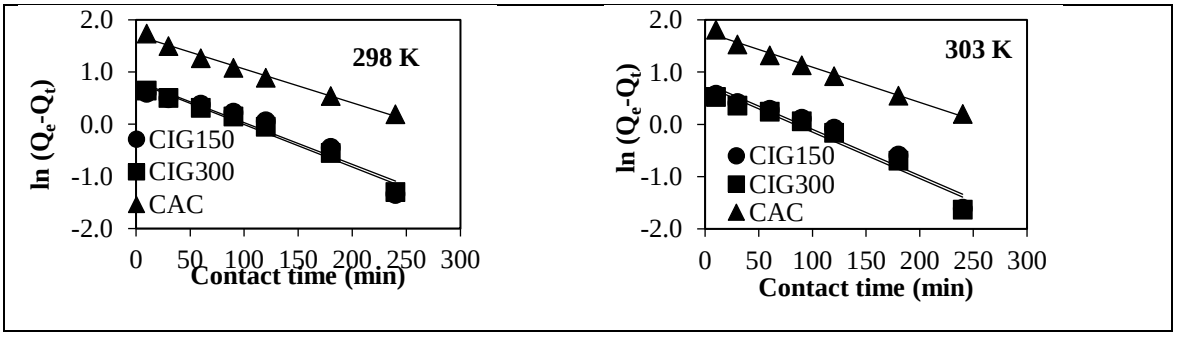


Figure 8: Lagergren Pseudo-first order Kinetic Plots for Removal of Chloride Ions from Wastewater by I. gabonensis Seed Shells Carbon (CIG150 = 150 µm; CIG300 = 300 µm Particle Size) and Commercial Activated Carbon (CAC)



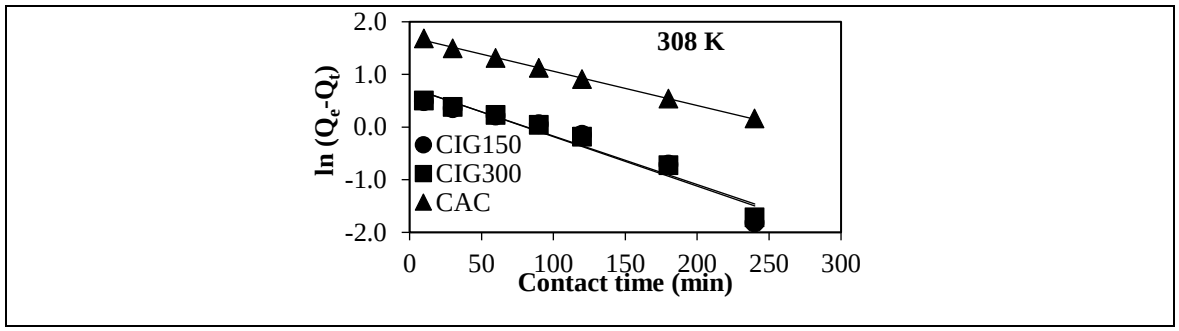


Figure 9: Lagergren Pseudo-first order Kinetic Plots for Removal of Sulphate Ions from Wastewater by I. gabonensis Seed Shells Carbon (CIG150 = 150 µm; CIG300 = 300 µm Particle Size) and Commercial Activated Carbon (CAC)

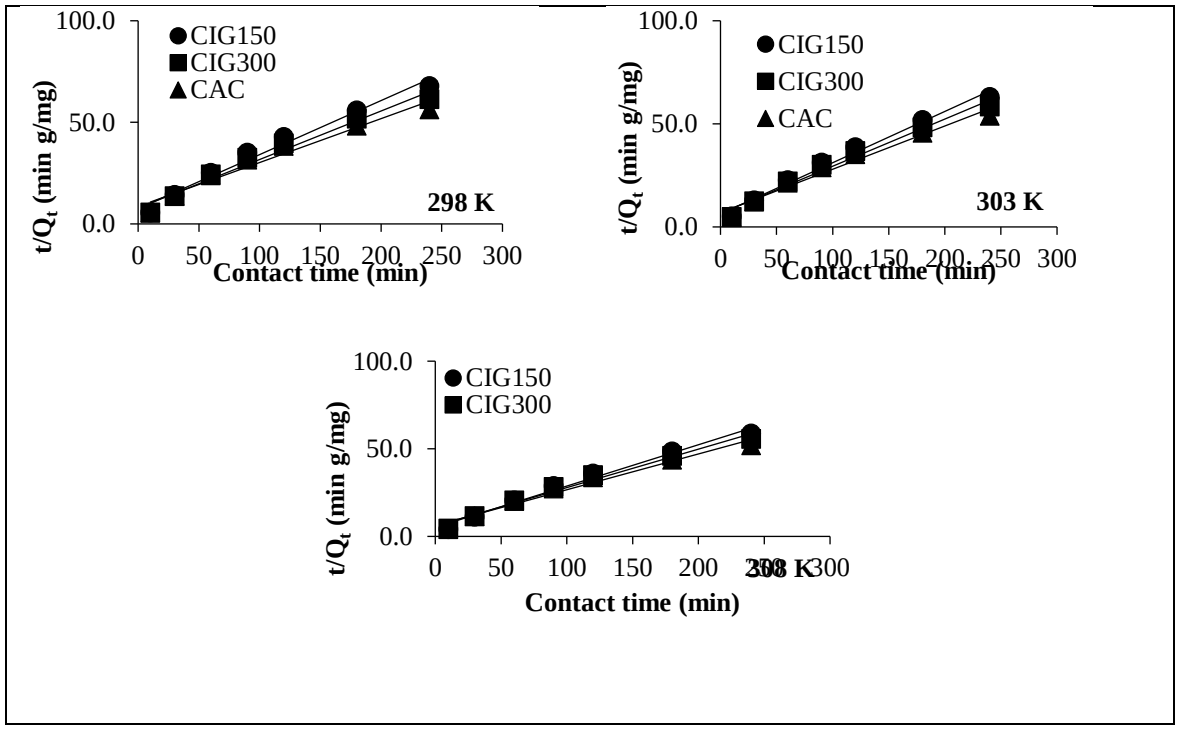
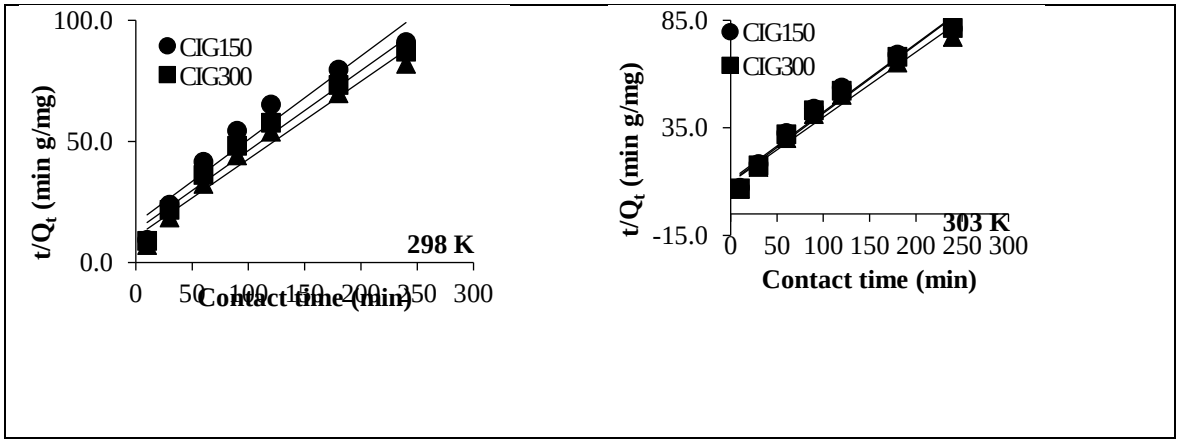


Figure 10: Blanchard Pseudo-second order Kinetic Plots for Removal of Chloride Ions from Wastewater by I. gabonensis Seed Shells Carbon



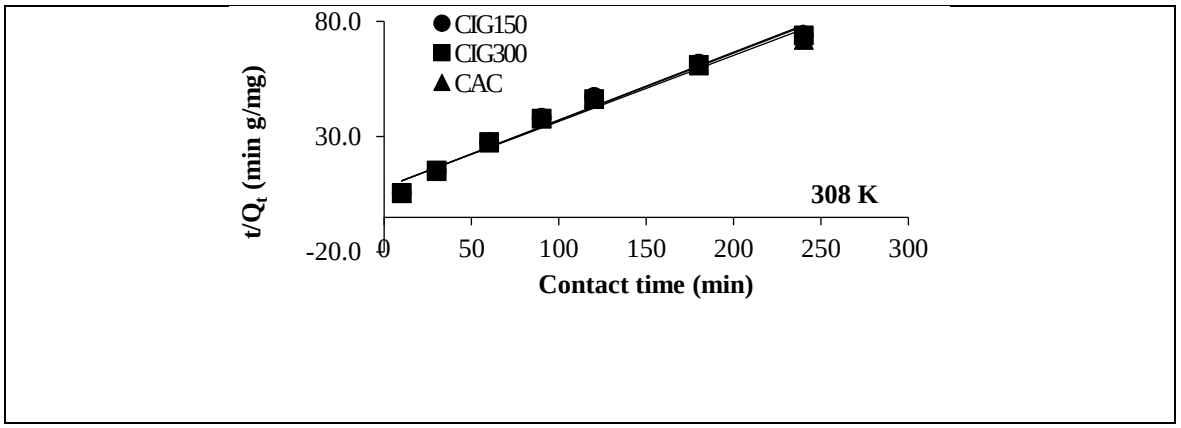


Figure 11: Blanchard Pseudo-second order Kinetic Plots for Removal of Sulphate Ions from Wastewater by I. gabonensis Seed Shells Carbon (CIG150 = 150 µm; CIG300 = 300 µm Particle Size) and Commercial Activated Carbon (CAC)

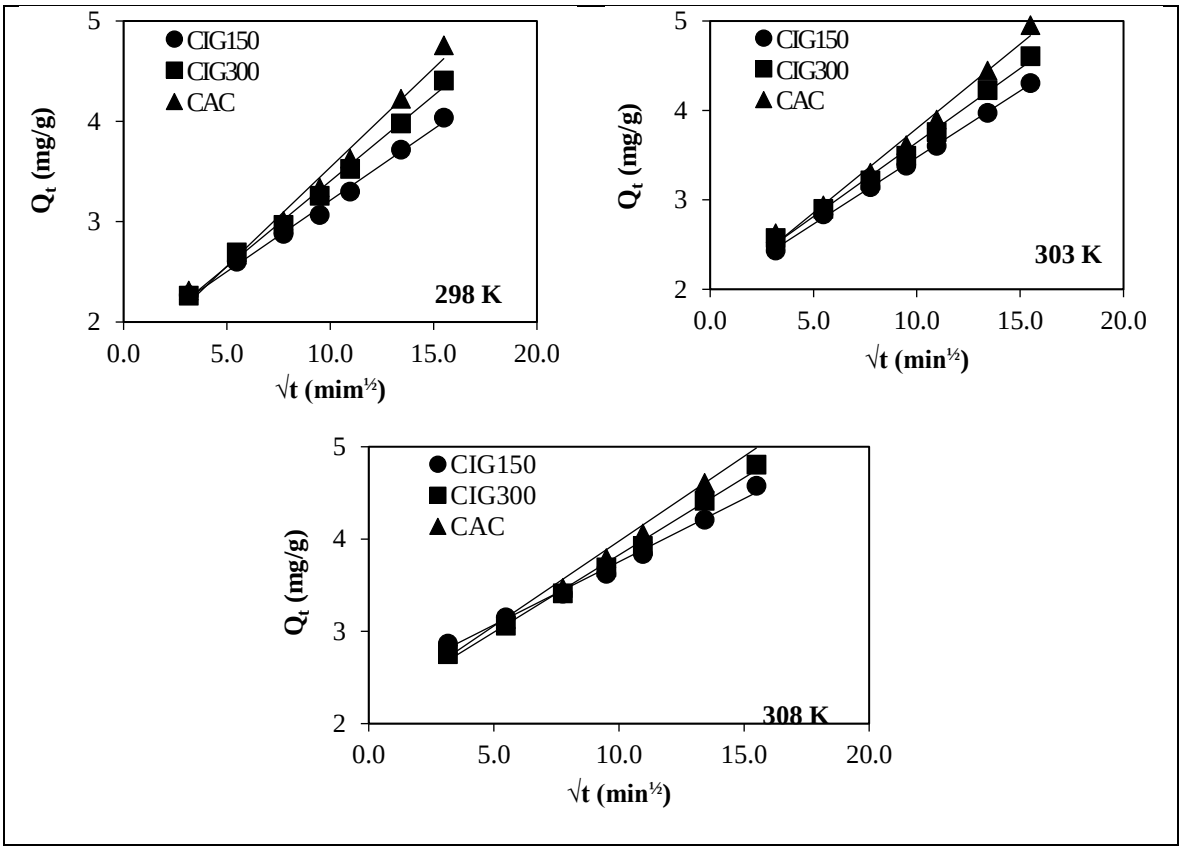


Figure 12: Weber-Morris Intra-particle Diffusion Plots for Removal of Chloride Ions from Wastewater by I. gabonensis Seed Shells Carbon (CIG150 = 150 µm; CIG300 = 300 µm Particle Size) and Commercial Activated Carbon (CAC)

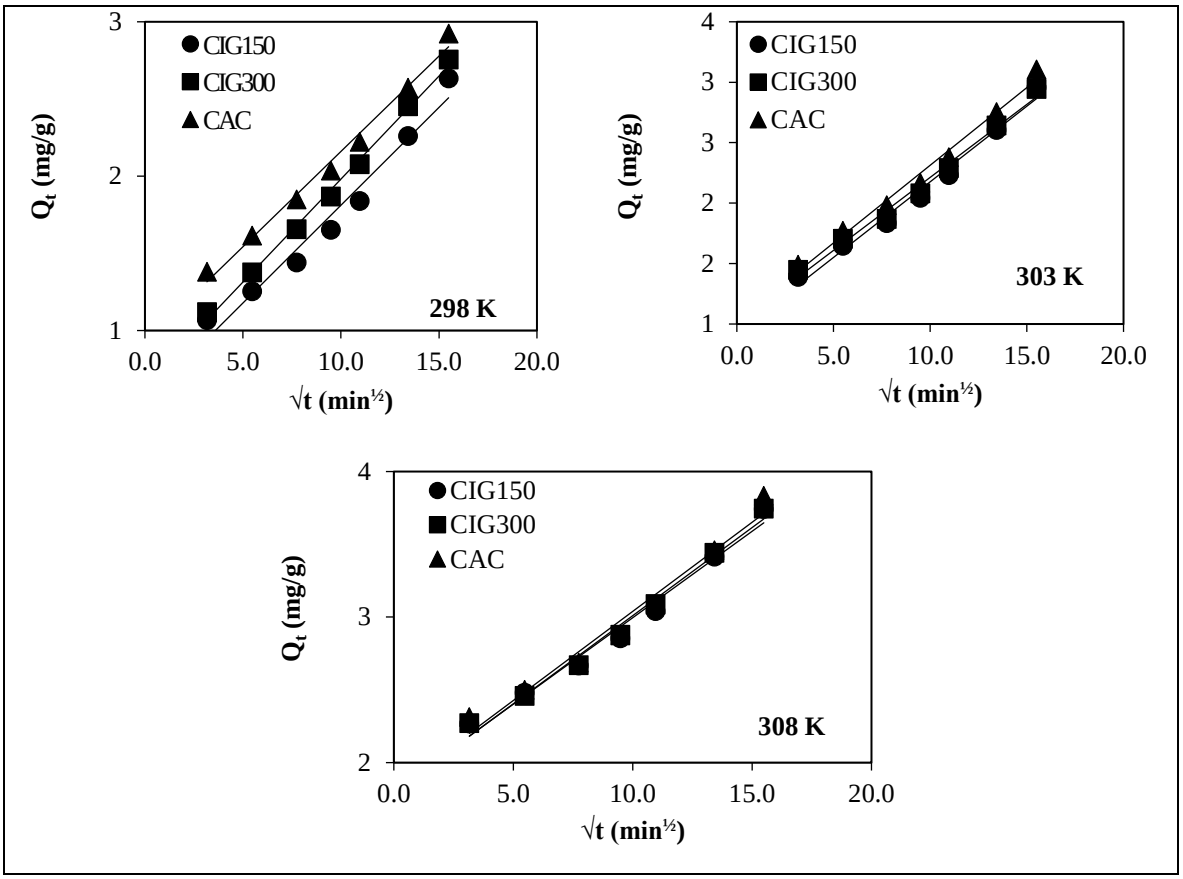


Figure 13: Weber-Morris Intra-particle Diffusion Plots for Removal of Sulphate Ions from Wastewater by I. gabonensis Seed Shells Carbon (CIG150 = 150 µm; CIG300 = 300 µm Particle Size) and Commercial Activated Carbon (CAC)

Table 3: Kinetic Parameters for Adsorption of Chloride and Sulphate Ions on Carbonized Irvingia gabonensis Seed Shells (CIG150 and CIG300) and Commercial Adsorbent (CAC) at Different Temperatures

Adsorbate	Adsorbent	Kinetic model	298 K	303 K	308 K
Chloride	CIG150	Lagergren - k_1 (min^{-1})	0.0091	0.0093	0.0099
		R^2	0.9640	0.9686	0.9361
		Blanchard - k_2 $(g.mg^{-1}min^{-1})$	0.0094	0.0099	0.1078
		R^2	0.9790	0.9852	0.9850
		Weber-Morris: k_{id} ($mg.g^{-1}min^{-½}$)	0.1490	0.1421	0.1368
		R^2	0.9947	0.9989	0.9928
	CIG300	Lagergren - k_1 (min^{-1})	0.0088	0.0090	0.0092
		R^2	0.9612	0.9667	0.9608
		Blanchard - k_2 $(g.mg^{-1}min^{-1})$	0.0073	0.0079	0.0081
		R^2	0.9739	0.9791	0.9806
		Weber-Morris: k_{id} ($mg.g^{-1}min^{-½}$)	0.1705	0.1673	0.1656
		R^2	0.9950	0.9950	0.9948
	CAC	Lagergren - k_1 (min^{-1})	0.0065	0.0067	0.0065
		R^2	0.9907	0.9895	0.9986
		Blanchard - k_2 $(g.mg^{-1}min^{-1})$	0.0054	000.63	0.0067
		R^2	0.9601	0.9702	0.9729
		Weber-Morris: k_{id} ($mg.g^{-1}min^{-½}$)	0.1972	0.1887	0.1838
		R^2	0.9866	0.9881	0.9840
Sulphate	CIG150	Lagergren - k_1 (min^{-1})	0.0080	0.0089	0.0094
		R^2	0.9416	0.9414	0.9325
		Blanchard - k_2 $(g.mg^{-1}min^{-1})$	0.0073	0.0093	0.0109
		R^2	0.9402	0.9673	0.9762
		Weber-Morris: k_{id} ($mg.g^{-1}min^{-½}$)	0.1267	0.1251	0.1188
		R^2	0.9698	0.9849	0.9804
	CIG300	Lagergren - k_1 (min^{-1})	0.0081	0.0089	0.0092
		R^2	0.9766	0.9595	0.9514
		Blanchard - k_2 $(g.mg^{-1}min^{-1})$	0.0082	0.0102	0.0109
		R^2	0.9673	0.9728	0.9790
		Weber-Morris: k_{id} ($mg.g^{-1}min^{-½}$)	0.1334	0.1211	0.1208
		R^2	0.9960	0.9869	0.9858
	CAC	Lagergren - k_1 (min^{-1})	0.0065	0.0067	0.0065
		R^2	0.9907	0.9895	0.9986
		Blanchard - k_2 $(g.mg^{-1}min^{-1})$	0.0097	0.0095	0.0101
		R^2	0.9696	0.9709	0.9728
		Weber-Morris: k_{id} ($mg.g^{-1}min^{-½}$)	0.1285	0.1235	0.1225
		R^2	0.9886	0.9878	0.9721

Similarly, the range of kinetic parameters for sulphate-CIG150, sulphate-CIG300 and sulphate-CAC sorption systems were respectively recorded thus: $0.80 \leq k_1(\times 10^{-2}) \leq 0.94$, $0.73 \leq k_2(\times 10^{-2}) \leq 1.09$, $11.88 \leq k_{id}(\times 10^{-2}) \leq 12.67$; $0.81 \leq k_1(\times 10^{-2}) \leq 0.92$, $0.82 \leq k_2(\times 10^{-2}) \leq 1.09$, $12.08 \leq k_{id}(\times 10^{-2}) \leq 13.34$; $0.65 \leq k_1(\times 10^{-2}) \leq 0.67$, $0.95 \leq k_2(\times 10^{-2}) \leq 1.01$, $12.25 \leq k_{id}(\times 10^{-2}) \leq 12.85$ across the temperatures.

DISCUSIONS

Effect of Initial Solution pH on Adsorption of Chloride Ions

The results of the effect of initial solution pH as depicted in Figure 2 demonstrate that, initial solution pH significantly influenced the adsorption of both chloride and sulphate ions by the three adsorbents. The observed changes in adsorption capacity with pH can be attributed to changes in the surface charge of

the adsorbents, the degree of ionization of surface functional groups and the aqueous speciation of the adsorbate ions. Solution pH is therefore an important parameter governing electrostatic interactions between adsorbate ions and active sites on an adsorbent (Utange *et al.*, 2021).

Overall, the results indicate that the pH conditions favouring adsorption were adsorbent- and ion-dependent. The optimum conditions for chloride removal were approximately neutral, whereas sulphate removal exhibited optimum conditions ranging from near-neutral to mildly alkaline pH. This difference demonstrates that the adsorption behaviour of the two anions was not identical and was influenced by their different physicochemical characteristics as well as the surface properties of the individual activated carbons.

Effect of Adsorbent Dosage on Adsorption of Chloride and Sulphate Ions

The uptake of chloride and sulphate ions per unit mass of adsorbent (CIG150, CIG300 and CAC) decreased with increase in the adsorbent dosage for all adsorbents at all the temperatures (Figures 3 – 4). This may be explained on the basis of mass balance (Equation 1). As adsorbent dosage is increased and the initial solution concentration is fixed as well as volume of solution, the available chloride or sulphate molecules are not enough to cover all the active adsorption sites on the adsorbent, resulting in low adsorbate uptake. The results of this study agree with works reported by Wuana *et al.* (2016).

Langmuir Isotherm Models for Adsorption of Chloride and Sulphate Ions

The isotherm profiles provide information regarding the nature and mechanism of adsorption for each adsorbate-adsorbent system. Equilibrium data from adsorption experiments are often presented graphically (in the form of an isotherm), which displays the ratio of sorbed to non-sorbed solute per unit mass of the adsorbent at constant temperature (Wuana *et al*., 2016). One of the assumptions of Langmuir model posits that adsorption occurs at homogeneous sites and forms a monolayer (Wuana *et al*., 2016). Similar to study reported by Utange *et al.* (2021), the Langmuir parameters considered at temperatures of interest (Table 1) were the maximum adsorption capacity corresponding to a monolayer coverage on the adsorbent surface (Q_m, mg/g), the Langmuir constant (K_L, L/mol) and a dimensionless equilibrium parameter called separation factor (R_L) used to indicate the nature of adsorption to be either unfavourable, linear, favourable or irreversible. The results in this study show that, the maximum adsorption capacity, Q_m, for all the adsorbate-adsorbent systems increased with increasing temperatures. As revealed, the chloride-adsorbent and sulphate-adsorbent systems had high Q_m values indicating the potency of the adsorbents in the order of CAC>CIG300>CIG150 at all temperatures studied. The adsorption of chloride and sulphate ions for all the adsorbents had R_L values within $0<R_L<1$ range, signifying favourable adsorption (Wuana *et al*., 2016).

Thermodynamic Considerations

The thermodynamic parameters evaluated for the aqueous phase removal of the chloride and sulphate ions by CIG150, CIG300 and CAC as presented in Table 2 show negative values of Gibbs free energy (ΔG^o) for the adsorption of chloride and sulphate ions onto CIG150, CIG300 and CAC. This can be attributed to the spontaneous nature of the adsorption process (Das *et al.*, 2014). The values of ΔG^o were found to decrease with increasing temperature, indicating that the spontaneity

and thermodynamic favourability of the adsorption process increased with increasing temperature (Tran *et al.*, 2017). Haro *et al.* (2021) reported a similar trend in their finding. As reported by Wuana *et al*. (2015), ΔG^o values in the range of -20.00 ≤ ΔG^o(kJ/mol) ≤ 0.00 represent physisorption, while those in the range of -400.00 ≤ ΔG^o(kJ/mol) ≤ -80.00 indicate chemisorption. The ΔG^o values of this study are suggestive of physisorption.

The negative values of enthalpy change (ΔH^o) i.e. -34.5529, -8.1094and -10.6660 kJmol^{-1} for chloride-CIG150, chloride-CIG300 and chloride-CAC systems respectively; -3.6390, -32.2998 and -7.3653 kJmol^{-1} for sulphate-CIG150, sulphate-CIG300 and sulphate-CAC sorption systems respectively, can be ascribed to the exothermic nature of the adsorption Process. As reported by Wuana *et al*. (2015), the magnitude of enthalpy values give an idea about the type of sorption stressing that, enthalpy change values in the range of $2.1 \leq \Delta H^o$(kJmol^{-1})≤ 20.9 signify physical adsorption while $80 \leq \Delta H^o$(kJmol^{-1})≤ 200 kJmol^{-1} imply chemical adsorption. The results of the present study for the adsorption of chloride and sulphate ions on CIG150, CIG300 and CAC are typical of physical adsorption.

The positive values of standard entropy change (ΔS^o) for the chloride-CIG300, chloride-CAC, sulphate-CIG150, sulphate-CAC sorption systems signify spontaneous nature of the adsorption of these species onto the adsorbents; reflect the affinity of the adsorbents towards the ions and also suggest increased randomness at the solid-liquid interface with some structural changes in the adsorbates/adsorbents (Wuana *et al*., 2015). It suggests an overall increase in disorder at the adsorbent-adsorbate interface during the adsorption process. This may be associated with the release of solvent molecules, increased translational freedom of adsorbate species (Xue *et al., 2024)* and possibly contribution from desorption following prolonged contact time. However, the entropy change (ΔS^o) for the chloride-CIG150 sorption system was negative suggesting that the adsorption process was enthalpy driven and also implies a decreased disorder at the solid-liquid interface during the adsorption process causing the chloride molecules to escape from the solid phase to the liquid phase, leading to a decrease in the amount of chloride ions adsorbed (Dawood, 2025).

Adsorption kinetic models

The order of magnitude of the kinetic parameters of all the adsorbate-adsorbent sorption systems across the temperatures varied thus: $k_{id}(\times 10^{-1}) > k_2(\times 10^{-3}) \approx k_1(\times 10^{-3})$. The experimental values of k_1 did not follow a regular pattern for all the sorption systems, possibly the kinetic data were not well modelled by the Lagergren pseudo-first-order model. The values of k_2 however, increased with increasing temperature for the Blanchard pseudo-second-order model while k_{id} values for the Weber-Morris intra-particle diffusion model decreased with increasing temperature (Das *et al*., 2014; Wuana *et al*., 2016; Wuana *et al*., 2015).

The adsorption kinetics for all the sorption systems were better interpreted by the Weber-Morris intra-particle kinetic model since it recorded the highest values of the coefficient of determination, R^2 (Wuana *et al*., 2016) although its linear plots did not pass through the origin. Das *et al*. (2014) opined that this kind of deviation from the origin is due to the difference in the rate of mass transfer in the initial and final stages of the sorption process, thus indicate the existence of some boundary layer effect and that Weber-Morris intra-particle kinetic model might not be the sole rate determining mechanism in the sorption process.

CONCLUSION

The uptake of chloride ions in the wastewater from an advanced chemistry laboratory recorded optimum pH of 6.8, 6.8, and 7.6 onto CIG150, CIG300 and CAC respectively. The uptake of sulphate ions on the other hand recorded optimum pH of 8.1 for CIG150 and 7.7 for both CIG300 and CAC. The adsorption capacity of the adsorbents under study however, decreased with increase in the adsorbent dosage. Langmuir isotherm model fitted the equilibrium data for the uptake of chloride and phosphate ions onto CIG150, CIG300 and CAC signifying that the adsorption occurs at homogeneous sites and that the maximum adsorption capacity increased with increase in temperature.

The thermodynamic parameters indicated that the uptake of chloride and sulphate ions onto CIG150, CIG300 and CAC were spontaneous, exothermic and physisorptive in nature. The adsorption kinetic data was well represented by the Weber-Morris intra-particle diffusion model. The adsorbents demonstrated good sorptive potency for the anions studied hence recommended for real wastewater treatment and that laboratories/related establishments could use these adsorbents in the preliminary treatment of aqueous effluents and wastewater from their operations before discharging into the environment especially when chloride and sulphate ions are in focus.

REFERENCES

Al-Qahtani, K. M. (2016). Water purification using different waste fruit cortexes for the removal of heavy metals. *Journal of Taibah University for Science*, ***10*****(5)**: 700–708. https://doi.org/10.1016/j.jtusci.2015.09.001

Berehanu, B., Lemma, B., and Tekle-giorgis, Y. (2015). Chemical composition of industrial effluents and their effect on the survival of fish and eutrophication of Lake Hawassa, Southern Ethiopia. *Journal of Environmental Protection*,***6***: 792–803.

Bernardi, E., Vassura, I., Raffo, S., Nobili, L., Passarini, F., de la Fuente, D. and Morcillo, M. (2020). Influence of inorganic anions from atmospheric depositions on weathering steel corrosion and metal release. *Construction and Building Materials*, 236: 117515. https://doi.org/10.1016/j.conbuildmat.2019.117515

Cao, Z., Hibino, M., and Goda, H. (2013). Effect of nitrite ions on steel corrosion induced by chloride or sulfate ions. *International Journal of Corrosion*, ***2013***: 1–16.

Cui, Y., Qin, Y., Dilimulati, D., and Wang, Y. (2019). The effect of chlorine ion on metal corrosion behavior under the scratch defect of coating. *International Journal of Corrosion*, ***2019***: 1–11. https://doi.org/https://doi.org/10.1155/2017/7982893

Das, B., Mondal, N. K., Bhaumik, R., and Roy, P. (2014). Insight into adsorption equilibrium, kinetics and thermodynamics of lead onto alluvial soil. *International Journal of Science and Technology*, ***11***: 1101–1114. https://doi.org/10.1007/s13762-013-0279-z

Dawood, I., Zyoud, A.H., Zyoud, S., Amireh, A., Zyoud, S.H. and Kim, T.W. (2025). Sustainable water purification through the adsorptive removal of tetracycline via modified clay and regeneration via controlled thermolysis: a reusable and environmentally friendly approach for contaminant mitigation. *Applied Water Science*, **15:**215. https://doi.org/10.1007/s13201-025-

02555-6

Dong, S.G., Du, R.G., Gao, Y.B., Liang, Y., and Guan, Z.C. (2017). Effect of Sulfate on Corrosion Behavior of Reinforcing Steel in Simulated Concrete Pore Solutions. *ECS Transactions*, ***75*(26)**: 17–23.

Ehalt Macedo, H., Lehner, B., Nicell, J., Grill, G., Li, J., Limtong, A. and Shakya, R. (2022). Distribution and characteristics of wastewater treatment plants within the global river network. *Earth System Science Data*, ***14***: 559-577.

Haro, N.K., Dávila, I.V.J., Nunes, K.G.P. de Franco, M.A.E., Marcilio, N.R. & Féris, L.A. 2021. Kinetic, equilibrium and thermodynamic studies of the adsorption of paracetamol in activated carbon in batch model and fixed-bed column. *Applied Water Science* 11: 38. https://doi.org/10.1007/s13201-020-01346-5

Ismail, A. (2014). Corrosion Behavior of Austenitic Stainless Steel in High Sulphate Content. *Advanced Materials Research*, ***893*(2014)**: 397–401. https://doi.org/10.4028/www.scienfiJic.net/AMR.893.397

Mesquita, R. B. R., Fernandes, S. M. V., & Rangel, A. O. S. S. (2002). Turbidimetric determination of chloride in different types of water using a single sequential injection analysis system. *Journal of Environmental Monitoring*, ***4***(3): 458–461. https://doi.org/10.1039/B200456A

Omowumi, A. (2018). Electrical resistivity and hydrogeochemical evaluation of septic-tanks effluent migration to groundwater. *Malaysian Journal of Geosciences*, ***2***(2): 1–10. https://doi.org/10.26480/mjg.02.2018.01.10

Phifer, R. (2024). The subtleties of managing laboratory waste in 2024. *ACS Chemical Health & Safety*, ***31***(6): 521-525. https://doi.org/10.1021/acs.chas.4c00047

Sahar, I. (2019). Waste management analysis from economic environment sustainability perspective. *International Journal of Scientific and Technology Research*, ***8*(12)**: 1540-1543.

Somashekara, D. and Mulky, L. (2023), Sequestration of Contaminants from Wastewater: A Review of Adsorption Processes. *ChemBioEng Reviews*, **10**(4): 491-509. https://doi.org/10.1002/cben.202200050

Song, Y., Jiang, G., Chen, Y., Zhao, P., and Tian, Y. (2017). Effects of chloride ions on corrosion of ductile iron and carbon steel in soil environments. *Scientific Reports*, ***7***: 1–13. https://doi.org/10.1038/s41598-017-07245-1

Spellman, F. R. (2020). *Handbook of water and wastewater treatment plant operations* (4th ed.). CRC Press. https://doi.org/10.1201/9781003038351

Tian, Y., Liu, Y., Yan, D., Xie, Y., Li, Y., Zhang, G., . . . Cai, Q. (2025). Coupled effects of chlorides and sulphates on steel reinforcement corrosion in concrete structures: A comprehensive review. *Case Studies in Construction Materials,* ***22:*** e04263. https://doi.org/10.1016/j.cscm.2025.e04263

Tran, H.N., You, S.J., Hosseini-Bandegharaei, A., Chao, H.P. (2017). Mistakes and inconsistencies regarding adsorption of contaminants from aqueous solutions: A critical review. *Water Research*, **120**: 88-116. doi:10.1016/j.watres.2017.04.014

Utange, P.I., Wuana, R.A. and Eneji, I.S. (2021). Preparation, Characterization and Evaluation of *Irvingia gabonensis*

Seed Shell Carbon for Sorptive Removal of Phosphate Ions in Wastewater. *FUW Trends in Science & Technology Journal*, ***6(1):*** 024 – 037 www.ftstjournal.com

World Health Organization. (2026). *Guidelines for Drinking-water Quality* (4th ed.). Malta: World Health Organization.

Wuana, R. A., Sha'Ato, R., and Iorhen, S. (2015). Aqueous phase removal of ofloxacin using adsorbents from Moringa oleifera pod husks. *Advances in Environmental Research*, ***4*(1)**: 49–68.

Wuana, R. A., Sha'Ato, R., and Iorhen, S. (2016). Preparation, characterization, and evaluation of *Moringa oleifera* pod husk adsorbents for aqueous phase removal of norfloxacin. *Desalination and Water Treatment*, ***57*(2016)**: 11904–11916. https://doi.org/10.1080/19443994.2015.1046150

Xue, J., Ji, M., Lu, Y., Pan, D., Yang, X., Yang, Z. and Xu, Z. (2024). The impact of chemical properties of the solid-liquid-adsorbate interfaces on the entropy-enthalpy compensation involved in adsorption. *Physical Chemistry Chemical Physics*, **26**(11): 8704-8715. https://doi.org/10.1039/d3cp05669d

Zhang, Y., Zhao, J., Jiang, Z., Shan, D., and Lu, Y. (2014). Biosorption of Fe (II) and Mn (II) ions from aqueous solution by rice husk ash. *BioMed Research International*, ***2014***: 1–10. https://doi.org/10.1155/2014/973095

Zhou, W., Lan, W., Cao, X., Deng, H., Yan, Y., and Hou, X. (2018). Effect of a high concentration of chloride ions on the corrosion behaviour of X80 pipeline steel in 0.5 mol/L sodium bicarbonate solution. *International Journal of Electrochemical Science*, ***13***: 1283–1292. https://doi.org/10.20964/2018.02.03